ISSN: 3068-2789

Research Article

Journal of All Physics Research and Applications

Mathematical Vibration Model of a Tank Gun Recoil System

Gnanasrenivash NB[1*], Saayan Banerjee[2], Mohanaharish V[3], Srinivasan G[4], and Rajesh Kumar J[5]

[1]*Scientist B, Centre for Engineering Analysis and Design CVRDE, DRDO, Chennai, India*

[2]*Scientist F, Centre for Engineering Analysis and Design CVRDE, DRDO, Chennai, India*

[3]*Student, PSG Institute of Technology and Applied Research, Coimbatore, India*

[4]*Scientist-G & Addl. Director, Centre for Engineering Analysis and Design CVRDE, DRDO, Chennai, India*

[5]*Scientist-H & Director, CVRDE, DRDO, Chennai, India*

[*]Corresponding author:
Gnanasrenivash N B, Scientist B, Centre for Engineering Analysis and Design CVRDE, DRDO, Chennai, India.

Abstract

This paper focuses on developing a detailed vibration mathematical model of a gun recoil system, which is used on Armored Fighting Vehicles (AFVs). An existing recoil system of a tank gun is considered for developing the vibration models, which is subsequently coded in MATLAB as well as in Simscape Fluids. The recoil system is modeled as a single degree of freedom mass, spring and damper system, which is subjected to external time variant firing force. However, unlike conventional vibration models, in this case, the non-linear fluid mechanics equations are incorporated across different flow paths of the fluid through fixed and variable length orifices to arrive at the actual damping force during the recoil and recuperation phase. These non-linear fluid mechanics equations are integrated with the single degree of freedom vibration mathematical model to determine the recoil distance, recoil and recuperation velocity as well as the transmitted force magnitude. Suitable conditional statements are incorporated in the MATLAB code to represent the fluid flow phenomenon across the variable length and fixed orifice regions. The same is established in Simscape Fluids by using appropriate blocks. The developed non-linear single degree of freedom vibration mathematical model responses is validated successfully with relevant experimental findings. This study has established a very vital platform for design and development of recoil system variants for light weight armoured platforms, which can further be used for evaluating the vehicle stability. This present research provides deep insight towards designing and optimizing advanced recoil systems for armoured vehicle platforms.

Keywords: Recoil, Recuperation, Single Degree of Freedom, Damping, Armoured Fighting Vehicle.

Received: January 16, 2026;
Accepted: January 24, 2026;
Published: January 31, 2026

Nomenclature

Aeq Effective area over which the pressure drop occurs across orifice g
A01 Area of cross section of single orifice in the floating shuttle/ spring seating area
A02 Area of cross section of single inclined orifice
A03 Area of cross section of single orifice near the dashpot
A04 Area of cross section of annular orifice
Afq Fluid flow area of the orifice g
a Acceleration of piston
Cd Coefficient of discharge of orifice
d Diameter of spring coil
D Overall diameter of spring
Dt Inner diameter of buffer cylinder
Dd Diameter of dashpot cylinder
dd Diameter of dashpot piston
fr Flow friction factor
G Shear modulus
Fi Inertia force of recoiling mass
Fdp Force exerted by dashpot in a single buffer cylinder
Frb Force exerted by recoil brake in a single buffer cylinder
Fr Force exerted by recuperator in a single buffer cylinder

Citation: Gnanasrenivash NB, Saayan Banerjee, Mohanaharish V, Srinivasan G, Rajesh Kumar J (2026) Mathematical Vibration Model of a Tank Gun Recoil System. J All Phy Res Appli 2: 1-11.

Fp Force exerted on piston due to fluid pressure developed during operation
Ff External firing force
Ft Force transmitted to structure
Fdi Damping force corresponding to pressure drop Δpi
Fdp Damping force due to dashpot
Fdps Damping force due to dashpot in Simscape fluids model
IDL Internal diameter of larger portion of gradual area change region
IDS Internal diameter of smaller portion of gradual area change region
k stiffness coefficient of spring
ki stiffness coefficient of j^{th}spring
K Effective stiffness coefficient of springs
l_o Length of varying diameter portion of control rod
l_m Length of micron annular orifice
lpd Length of dashpot piston
m Mass of recoiling parts
n No. of active coils of spring
n_01 No. of peripheral orifices in floating shuttle/ spring seating area
n_02 No. of peripheral inclined orifices
n_03 No. of peripheral orifices before dashpot
Δpq Pressure drop across the orifice g
r_o1 Radius of orifice in floating shuttle/ spring seating area
r_o2 Radius of inclined orifice
r_o3 Radius of orifice near dashpot
ron2 Radius of inclined orifice in the normal direction of fluid flow
rc1 Radius of control rod tip
rc1x Radius of control rod at the fluid entry region for piston displacement x
rc2 Radius of control rod root
rcm Mean radius of control rod
rm1 Inner radius of micron annular orifice
rm2 Outer radius of micron annular orifice
rp1 Radius of solid portion piston
rp2 Radius of piston covering the periphery of inclined orifices measured on the piston outer side
rp3 Inner radius of annular portion of piston tube
rp4 Radius of piston covering the periphery of inclined orifices measured on the inner side
rp5 Radius of opening in the piston head/ outer radius of annular orifice
rp6 Outer radius of hollow portion of piston
rp7 Outer radius of the annular orifice measure at the entry of fluid flow during recuperation
rp8 Radius of dashpot cylinder t Time
Δt Time increment
V Velocity of piston
x Displacement of piston of recoil system
p Density of hydraulic fluid
μ Dynamic viscosity of fluid
v Kinematic viscosity of fluid
α Control rod taper angle
θ Semi cone angle of gradual area change/ inclined orifices Subscripts
g =1 orifices in floating shuttle/ spring seating area during recoil
g =2 inclined orifices during recoil
g =3 long varying area annular orifice during recoil
g =4 orifices before dashpot during recoil when the displacement is less than *lo*
g =5 orifices before dashpot during recoil when the displacement is more than *lo*
g =6 micron annular orifice during recoil
g =7 annular orifice during recuperation
g =8 inclined orifices during recuperation
g =9 orifices in floating shuttle/ spring seating area during recuperation
g =10 orifices near dashpot during recuperation
g =11 micron annular orifice during recuperation

Introduction

When ammunition is fired from a gun, the pressure of gas developed inside the barrel, forces the ammunition towards the muzzle. This phenomenon exerts an equal and opposite force on the breech, which drives the gun backwards with a significant amount of force. The primary function of a recoil mechanism is to absorb this firing load and control the recoil movement of the gun assembly within desirable limit. In order to reduce the firing loads transmitted to the structure, the recoil system can be designed to allow for a long recoil movement over which the recoil force can be absorbed. But in case of tanks & armoured vehicles, the recoil distance is often limited by the space available inside them. Hence, the recoil mechanism should absorb and transmit the recoil loads within limited recoil distance. Mathematical modelling of such gun recoil systems is essential for predicting performance, ensuring structural integrity, and enhancing firing accuracy. Early seminal work by Ho et al. laid the groundwork for hydro spring and hydro pneumatic recoil mechanisms using MATLAB/Simulink and mechanical-fluid coupling approaches [1]. Building on these principles, Turkmen and Celik modelled heavy-weapon hydro pneumatic recoil motion by deriving breech forces via LeDuc equations, incorporating hydraulic braking and recuperator forces, and validating recoil displacement and velocity with experimental data [2]. Szupieńko and Woźniak developed a mathematical model for automatic short-recoil firearms, capturing bolt recoil phases and linking model behaviour to SolidWorks simulations of recoil velocities [3]. Yang et al. proposed a time-dependent hydraulic recoil brake model accounting for an unfilled counter-recoil chamber, showing close agreement with test-derived recoil curves [4]. Lien et al. conducted numerical analysis on oil characteristics in hydraulic recoil braking systems, highlighting the role of oil compressibility and temperature effects on peak resistance and recoil length [5]. Tuan and Phu examined the influence of piston–cylinder clearance on recoil performance, demonstrating significant increases in recoil velocity and stroke when gap sizes exceeded 0.285 mm [6]. Meanwhile, Elsaady et al. introduced a recoiling-barrel design for adapting conventional mortars to vehicle platforms, achieving over 60% recoil force reduction and shortening recoil length to around 26 cm [7]. In the paper by Roy et al. [8], recoil systems are discussed in the context of improving gun performance, particularly for next-generation weaponry. The authors highlight the importance of effective recoil management to ensure firing stability and accuracy in high-energy systems. In this work, a comprehensive dynamic model of a tank gun recoil mechanism, integrating hydraulic damping, spring recuperation validated against experiments are discussed.

The present work focusses on development of a detailed non-linear mathematical vibration model and Simscape model of a recoil system by inclusion of the essential design parameters of the helical spring and damper such as orifice radii, variable lengths of the orifice, number of orifices and orifice orientations. Apart from inclusion of the important design parameters, the variations of internal dynamic phenomenon, occurring inside the recoil system at different positions of the piston, have been captured in both the models. This detailed model establishes the base platform to freeze the conceptual design of any recoil system. It forms a very novel and generic model and can be easily extended towards the design and development of light armoured platform recoil systems with split type configuration.

Gun Recoil Systems

A gun recoil mechanism primarily consists of three elements: a recuperator, a recoil brake and a dashpot. A recuperator is a device that stores a part of energy during recoil phase. It returns the recoiling parts to the battery during the counter recoil phase. Mechanical springs or gas filled chambers are used as a recuperator. There is always a force exerted by the recuperator to hold the recoiling parts in the battery position irrespective of the angle of elevation. The recoil brake absorbs energy during recoil. It consists of a piston, with multiple orifices, moving in a chamber filled with hydraulic fluid. The movement of the piston produces a restricting force, due to the pressure drop of the fluid when it flows through one or more orifices. The dashpot arrangement, works similar to a recoil brake which absorbs energy during counter recoil. The energy stored by the recuperator at the end of recoil is more than sufficient enough to bring the recoiling parts to the battery position at a considerable velocity. This force should be controlled by the dashpot to reduce the impact during counter recoil and reduce the weapon to nose over.

Components of Recoil System

The tank gun recoil system considered for this work, has a buffer cylinder, filled with hydraulic fluid and a piston that reciprocates inside the cylinder. The piston is preloaded with springs and positioned in a retracted state. The cylinder housing is fixed to the structure and the piston end is connected to the breech of the gun. During recoil and recuperation phase, the piston, along with the breech, moves back and forth inside the cylindrical housing. It is to be noted that there are two such identical cylinders positioned diagonally across the gun barrel in a parallel fashion. The cross-section view of the buffer cylinder is shown in Figure 1. Here, two helical compression springs connected in series act as the recuperator in a single cylinder. When the piston reciprocates, the springs compress and expand along with it. A floating shuttle is present at the center and connects the two springs in series. It slides over the piston and transfers the force from one spring to another.

The function of the recoil brake is achieved by a number of orifices in the piston, which produces damping when it moves in the fluid filled chamber. The piston is hollow and contains fluid in its both outer and inner region. There are a number of peripheral inclined orifices which connect the outer and inner region. The piston head has a circular opening and acts as a variable area annular orifice. The varying area is achieved by using a control rod fixed to the cylinder, whose cross- section area varies along the length. There is another set of peripheral orifices attached to the control rod. In addition to this, there is a dashpot type arrangement at the end of the control rod, to absorb the forces during the end of recuperation phase.

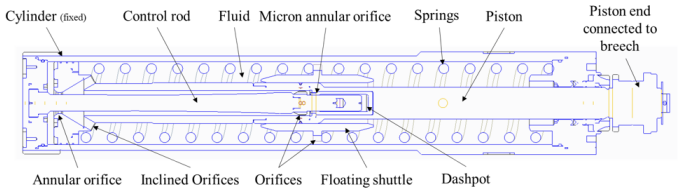

Figure 1: Cross-section view of a buffer cylinder

Approach To Mathematical Modelling

The recoil mechanism is modelled as a nonlinear, single degree of freedom mass, spring and damper system, subjected to external firing force. The total mass of the recoiling parts is considered as a single equivalent lumped mass. The recuperator is modelled as springs connected in series. The recoil brake and dashpot are modelled as dampers using fluid dynamic equations. The firing load is considered as external force acting on the system. The governing relation of a mass, spring, damper assembly subjected to external force is given by

Inertia force + Damping force + Spring force + Other forces = External firing force

In the case of the recoil system, the recoiling mass resists the motion and provides the inertia force; recoil brake and dashpot provide the damping force and recuperator provides the spring force. As mentioned earlier, the recoil system considered in this work has two identical buffer cylinders, each having a recuperator, recoil brake and a dashpot. In addition to the above forces, fluid pressure developed inside the cylinder during operation exerts an additional force on the piston. The corresponding force relation equation for recoil system model is given by Eq. (1).

$$F_i + 2\left(F_{rb} + F_{dp} + F_r\right) + F_p = F_f \quad (1)$$

Calculation of Inertia Force

The inertia force is given by Newton's second law of motion, which states that the force is equal to mass multiplied by acceleration. Here the inertia force of the recoil system is given by mass of the recoiling parts multiplied by the acceleration of the piston, as shown in Eq. (2).

$$F_i = ma = m\frac{d^2x}{dt^2} \quad (2)$$

Calculation of External Firing Force

The variation of pressure as a function of time, inside the gun barrel, during firing is measured from experiments. This internal pressure, when multiplied with the barrel's internal cross-section area gives the force acting on the projectile, which is also equal to the force acting on the recoil system, *Ff*.

Calculation of Recuperator Force

When the gun recoils, due to the recoil force *Ff*, the breech accelerates in the direction opposite to the direction of the projectile. The breech displaces the piston, which compresses

the two springs, connected in series to store energy. During recuperation, the spring expands releasing the energy stored to move the recoiling parts to the battery position.

The stiffness of individual springs and the effective stiffness of the springs in series is calculated by Eqs. (A1) and (A2) in appendix respectively. The recuperator force at any instant is obtained by multiplying the effective stiffness with instantaneous displacement of the piston as shown in Eq. (3)

$$F_r = K_x \tag{3}$$

On substituting the Eqs. (2) and (3) in Eq. (1), we get

$$m\frac{d^2x}{dt^2} + 2\left(F_{rb} + F_{dp} + Kx\right) + F_p = F_f \tag{4}$$

The solution of Eq. (4) gives displacement of the recoiling parts, x, as a function of time.

The mathematical model for the recoil system is developed using two methods. In first method, the model is developed by coding the governing equations of pressure drop and corresponding damping force of the orifices in MATLAB. In the second method, Simulink/Simscape fluids is used to build the recoil system by modelling the different elements of it using appropriate blocks for accurate representation of fluid flow dynamics and component interactions.

Mathematical Model Development Using Matlab Code

In this method, the recoil brake and dashpot forces are calculated by evaluating the pressure drop across the orifices and dashpot during the piston movement. The pressure drops when multiplied with the effective area over which it occurs gives the resistive force offered. The total resistive force is calculated by summing the forces across all the orifices

The following assumptions are considered for the purpose of simplifying the modelling procedure

a) Since, major pressure drop and damping is expected to occur across the orifices, the flow in other regions is considered to be laminar, to simplify the governing equations.

b) The flow is considered as fully developed flow.

c) The friction factor is assumed to be zero. Wall friction losses are neglected under the assumption that pressure drop across the orifices are significant. This simplification is appropriate for short flow paths or configurations

d) The value of discharge coefficient of the orifices is constant. The fixed discharge coefficient value assumption provides a reasonable first approximation since experimental calibration data are unavailable.

e) For different positions of piston during recoil and recuperation, only those orifices contributing to significant damping are considered. The damping due to remaining orifices, at that instant, is considered to be negligible.

Initial conditions & displacement, velocity and acceleration relations

The system is stationary before firing. Therefore, the two initial conditions i.e. initial displacement and initial velocity of the system, for solving the second order differential equation Eq. (4), are considered as zero.

$$x(t = 0) = 0 \tag{5}$$

$$v(t = 0) = 0 \tag{6}$$

The instantaneous displacement (x), velocity (v) and acceleration (a) of the piston at any time step t and subsequent time step ($t + \Delta t$), are related by following Eqs. (7) and (8)

$$x\,(t + \Delta t) = (t) + x(t)\,\Delta t \tag{7}$$

$$v(t + \Delta t) = v(t) + v(t)\,\Delta t \tag{8}$$

The sign convention for the displacement is considered to be positive when the piston moves in the recoil direction as shown Figure 2.

Calculation of Effective Damping Force by Recoil Brake and Dashpot

The damping force is offered by the fluid resistance when it flows across the orifices. This force is evaluated by calculating the pressure drop occurring across each orifice and multiplying it with the corresponding effective area, over which the pressure drop occurs. The effective damping force of the system is the sum of the damping forces across the individual orifices at that particular instant of time. The flow path of the fluid is different during recoil phase and recuperation phase. Therefore, the damping force is calculated by individually considering the recoil and recuperation phase separately.

Damping Force during Recoil Phase: During recoil phase, the movement of the piston forces the fluid to flow from the outer region, through orifices in the floating shuttle and inclined orifices, into the inner region. The flow then splits into two paths. One flows into the annular orifice, whose orifice area varies with the piston stroke and fills the cylinder volume on the left side of piston. The remaining fluid passes through an annular gap acting as a varying area long annular orifice, formed between the control rod and the inner wall of the piston. Further, this part of the fluid passes through another set of orifices, a micron annular orifice and finally fills the dashpot. The flow direction during recoil inside the cylinder is marked in red arrows as shown in Figure 2. The recoil phase is considered whenever the velocity of the piston is positive i.e. $v(t) > 0$

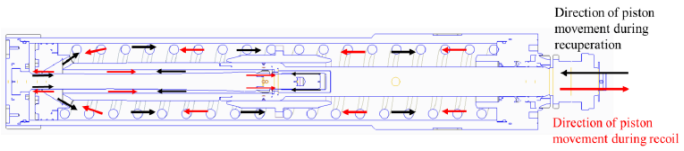

Figure 2: Fluid flow direction inside the cylinder during recoil phase and recuperation phase

When recoil starts, the fluid in the outer region flows to the inner region through number of semicircular orifices in the floating shuttle/ spring seating area. The pressure drop across these orifices is calculated by Eq. (B1) in appendix and damping force is calculated by Eq. (9)

$$F_{d1} = \Delta p_1 A_{e1} = \Delta p_1 \left(\frac{\pi}{4} D_t^2 - \pi r_{p1}^2\right) \tag{9}$$

Then, the fluid passes through inclined orifices attached to the piston. The pressure drops across these orifices is calculated by Eq. (B2) in appendix and damping force is calculated by Eq. (10).

$$F_{d2} = \Delta p_2 A_{e2} = \Delta p_2 \left(\frac{\pi}{4} D_t^2 - \pi r_{p2}^2\right) \quad (10)$$

These two orifices contribute to the damping all the time, irrespective of the position of the piston.

After passing through the inclined orifices, a portion of fluid enters into the long varying area annular orifice. The length of the region of the control rod where diameter is varying is l_0. Only when the displacement of the piston is less than l_0, the pressure drop of this region will contribute to the damping. Assuming the radius of the control rod varies linearly from start to end, the taper angle is given by α. The radius of control rod as function of distance, r_{c1x} is evaluated. The pressure drops occurring due to the long variable area orifice is calculated using Hagen Poiseuille's equation given by Eq. (B3) in appendix and the corresponding damping force is given by Eq. (11).

$$F_{d3} = \Delta p_3 A_{e3} = \Delta p_3 \left(\frac{\pi}{4} D_t^2 - \pi r_{p2}^2\right) \quad (11)$$

After long varying area annular orifice, the fluid flows across peripheral semicircular orifices before the dashpot. From the initial piston position, till the piston head displaces up to l_0, the flow enters through the varying area annular orifice. The pressure drop is given by Eq. (B4) in appendix and damping force during this condition is given by Eq. (12).

$$F_{d4} = \Delta p_4 A_{e4} = \Delta p_4 \left(\frac{\pi}{4} D_t^2 - \pi r_{p2}^2\right) \quad (12)$$

When the piston displaces beyond l_0, the flow directly goes into these orifices. In this condition, the pressure drop is given by Eq. (B5) in appendix and damping force is given by Eq. (13).

$$F_{d5} = \Delta p_5 A_{e5} = \Delta p_5 \left(\frac{\pi}{4} D_t^2 - \pi r_{p2}^2\right) \quad (13)$$

The micron orifice's annular region is formed by the overlap of dashpot's piston and inner cylindrical hole in the piston. This overlap happens from the initial position of the piston till it displaces by l_{pd} which is the length of the extended cylindrical rod. Therefore, the pressure drop contributed by this orifice will be applicable only during the phase when the displacement is less than l_{pd}. As the piston displaces beyond l_{pd}, the fluid flows directly into the dashpot. The pressure drop is calculated using Hagen Poiseuille's equation given by Eq. (B6) in appendix and the damping force is given by Eq. (14).

$$F_{d6} = \Delta p_6 A_{e6} = \Delta p_6 \left(\frac{\pi}{4} D_t^2 - \pi r_{p2}^2\right) \quad (14)$$

Damping Force During Recuperation Phase: At the end of recoil phase, the compressed spring expands forcing the piston to the initial equilibrium position. Due to the movement of the piston, the fluid stored in the chamber volume is forced to flow across the annular orifice formed by the piston head and the control rod. Then the fluid flows from the inner region to the outer region through inclined orifices and peripheral orifices in the floating shuttle/spring seating area. At the end of recuperation phase, the fluid in the dashpot flows out through the micron orifice providing a cushioning effect. Then it flows to outer region through the long varying area orifice. The flow direction during recuperation inside the cylinder is marked in black arrows as shown in Fig. 2. The recoil phase is considered whenever the velocity of the piston is negative i.e., $v(t) < 0$

When the recuperation starts, the fluid is forced to flow through the annular orifice formed by the piston head and control rod. To account for the varying diameter of the control rod, mean diameter of its's ends is considered. The pressure drop is given by Eq. (B7) in appendix and damping across this orifice is given by Eq. (15).

$$F_{d7} = \Delta p_7 Ae_7 = \Delta p_7 \frac{\pi D_t^2}{4} \quad (15)$$

Then the fluid enters into the outer region through the inclined peripheral orifices. The pressure drop is given by Eq. (B8) in appendix and damping across this orifice is given by Eq. (16).

$$F_{d8} = \Delta p_8 A_{e8} = \Delta p_8 \frac{\pi}{4} D_t^2 \quad (16)$$

This part of fluid also passes through the orifices in the floating shuttle/spring seating area. The pressure drop is given by Eq. (B9) in appendix and damping across this orifice is given by Eq. (17).

$$F_{d9} = \Delta p_9 A_{e9} = \Delta p_9 \left(\frac{\pi}{4} D_t^2 - \pi r_{p6}^2\right) \quad (17)$$

These above orifices contribute to the damping all the time, irrespective of the position of the piston

Due to movement of the piston, fluid in the dashpot exits and passes through the peripheral orifices adjacent to the dashpot. The pressure drop in these orifices is significant only when the position of the piston is in such a way that there is no overlap of dashpot piston cylinder. This condition occurs when the displacement of the piston is greater than the l_{pd}. The pressure drop is given by Eq. (B10) in appendix and damping across this orifice is given by Eq. (18) respectively.

$$F_{d10} = \Delta p_{10} A_{e10} = \Delta p_{10} \left(\pi r_{p3}^2\right) \quad (18)$$

At the end of recuperation, complete fluid in the dashpot is forced out through the micron level orifice. As discussed earlier, the pressure drop contributed by the micron level orifice will be applicable only during the phase when the piston comes back to a position where the displacement is less than l_{pd}. The drop in pressure in this orifice is given by Eq. (B11) in appendix and damping force is given by Eq. (19).

$$F_{d11} = \Delta p_{11} A_{e11} = \Delta p_{11} \pi r_{p8}^2 \quad (19)$$

Total Effective Damping Force Due to Recoil Brake and Dashpot: The sum of damping forces due to all the orifices at a particular instant of time gives the total damping. The total damping force is given by Eq. (20)

$$F_{rb} + F_{dp} = \sum_{j=1}^{11} F_{dj} \quad (20)$$

Calculation of Piston Displacement and Transmitted Force

From the governing equation of motion Eq.(4), acceleration can be calculated by

$$\frac{d^2x}{dt^2} = \frac{(F_f - 2(F_{rb} + F_{dp} + Kx) - F_p)}{m} \quad (21)$$

Using the initial conditions Eqs. (5) and (6), Eq. (21) is solved to get the instantaneous acceleration at time step t. The velocity and displacement values corresponding to next time increment ($t + \Delta t$), is calculated by using the Eqs. (5,6).

The force transmitted to the structure during recoil and recuperation is given by the sum of forces due to the recuperator, recoil brake and dashpot given as shown in Eq. (22).

$$F_t = 2(F_{rb} + F_{dp} + F_r) + F_p \quad (22)$$

Mathematical Model Development Using Simulink/Simscape Fluids

In this approach, to analyze the dynamic behavior of the tank gun recoil system, a detailed simulation model is developed using Simulink/Simscape Fluids. The working of the recoil system is carefully analyzed and different components such as recoiling mass, recuperator, recoil brake, dashpot are broken down into corresponding blocks to accurately model, simulate their working and interaction with other components. By modelling these components into modular blocks, the Simscape environment enables a structured and scalable approach for simulating the entire system.

The following assumptions, similar to previous approach, are considered for the purpose of simplifying the modelling procedure

1. The flows are assumed to be in one dimension, for preliminary analysis.
2. The value of discharge coefficient of the orifices is constant. This assumption provides a reasonable first approximation since experimental calibration data are unavailable
3. The motion of walls of orifices is not considered.
4. The flow friction is assumed to be negligible, considering the pressure drop across the orifices are significant.

Overall Modelling Strategy of Recoil System in Simscape Fluids

In the Simulink/Simscape Fluids, individual blocks are created for modelling the mass, recuperator, recoil brake and dashpot. The mass block is connected to the ground structure through two parallel buffer cylinder blocks. Each buffer cylinder block has a recuperator, recoil brake and dashpot blocks representing a mass, spring, damper system. The recuperator block is connected in parallel with the recoil brake and dashpot blocks. The external input force block is connected to provide the firing force to the system. The overall schematic of Recoil system modelled in Simscape Fluids is shown in Fig. 3.

Modelling of External Input Force in Simulink/ Simscape Fluids

The input force is modelled using Ideal force source block which provides the firing force to the model. The firing force F_f, is fed into the model with the help of 1-D lookup Table and Translational Ideal force source blocks as shown in Figure 4. The force vs time values are fed into table data of lookup table and its output is fed into Ideal force source block. The simulation time from the Clock block is fed into lookup table to output the corresponding force value.

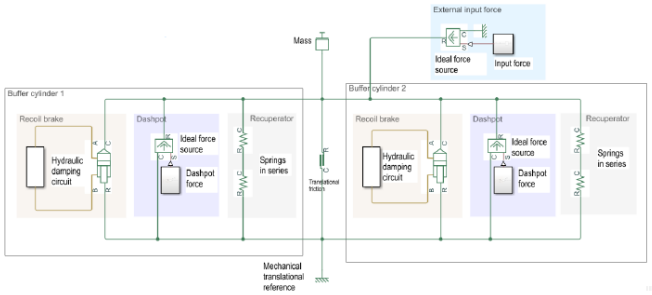

Figure 3: Overall schematic of Recoil system modelled in Simscape Fluids

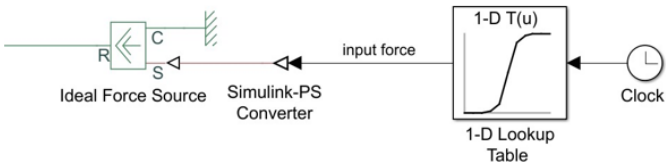

Figure 4: Input force using Ideal force source block

Modelling of mass and recuperator in Simulink/Simscape fluids The total mass of the recoiling components is modelled by an Ideal mechanical translational mass block. The recuperator i.e. two series springs is modelled by connecting two Ideal mechanical linear spring blocks in series as shown in Figure 3. The stiffness value of the spring, k is entered in the block parameter. To capture the effect of friction between the moving components of the recoil system, a Translational friction block is connected parallel to the cylinders.

Modelling of Recoil Brake in Simulink/Simscape Fluids

The recoil brake is modelled using a Double-acting hydraulic cylinder block. The block has two mechanical translational conserving ports corresponding to the piston rod & cylinder clamping structure and two hydraulic conserving ports. The two hydraulic conserving ports of the double acting cylinder are connected by a hydraulic circuit consisting of all the hydraulic damping elements of the recoil system. The hydraulic damping circuit is responsible for capturing the damping offered by the recoil brake. The different regions in the fluid flow path are modelled using different blocks as shown in Table 1. The hydraulic damping circuit of recoil brake is shown in Figure 5.

Table 1: Blocks used for modelling different regions of recoil brake

Region	Blocks used for modelling the region
Outer Annular region	Annular Orifice
Inclined Orifice region	Fixed Orifices

Gradual Area Change region	Simscape Component (Gradual Area Change)
Variable annular orifice region	Simscape Component (Annular Orifice)
Sudden Area Change region	Simscape Component (Sudden Area Change)

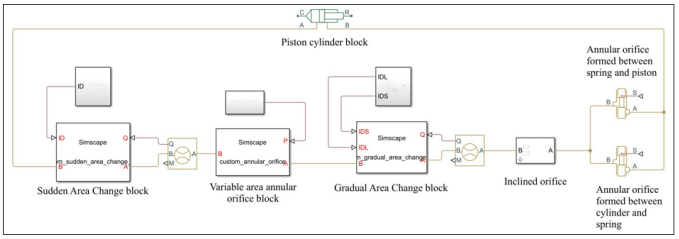

Figure 5: Hydraulic damping circuit of recoil brake

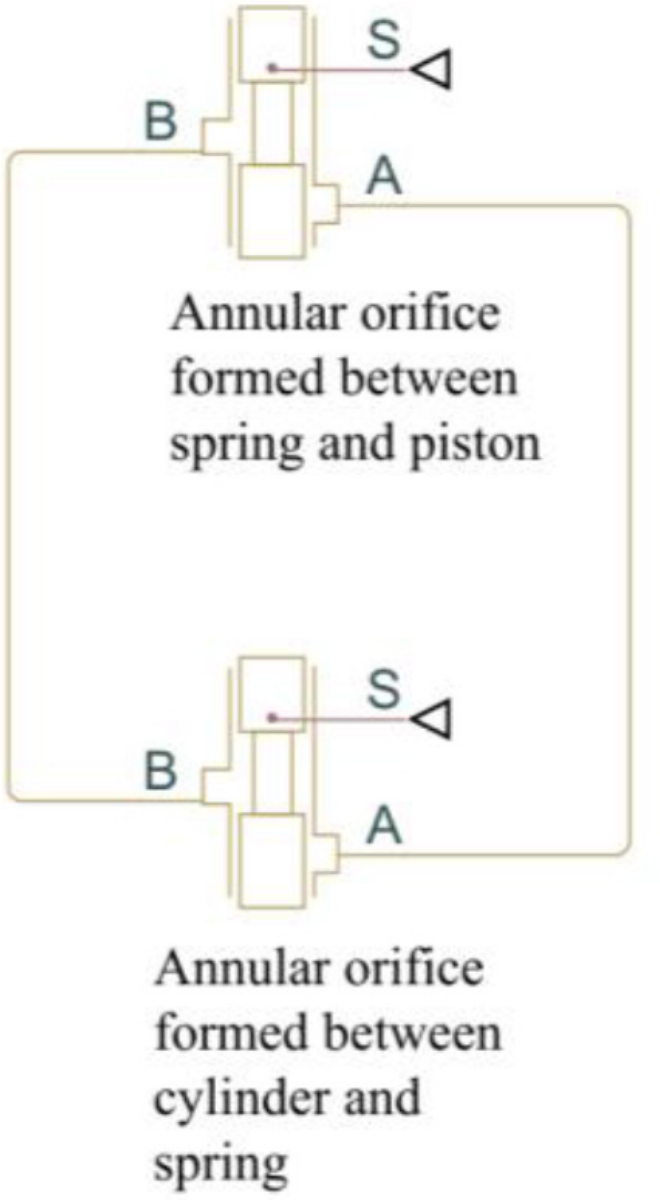

Figure 6: Simscape annular orifice blocks

Outer Annular Region: As the firing force acts on the piston, it displaces the oil in the region between the buffer cylinder and the piston. The fluid flows between the coils of the spring and enters into the main orifice. This complex flow is simplified and modelled as two annular orifice flow blocks. One annular flow is considered in the gap formed between spring and buffer cylinder and other annular flow is considered between the spring and piston. These two annular orifice blocks are then connected in parallel as shown in Figure 6. Similarly, during recuperation the fluid is forced to flow back in to the outer annular region through the inclined orifice.

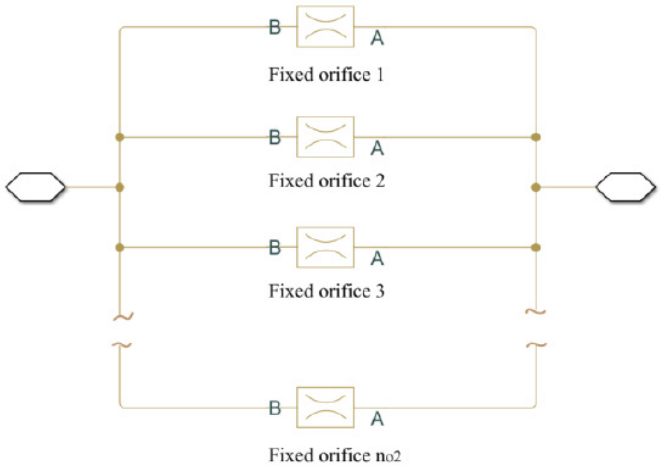

Figure 7: Simscape Fixed orifice blocks connected in parallel

Inclined Orifice Region: The oil flows through the inclined orifices during recoil and recuperation phase. This region is represented by a number of Fixed Orifice blocks connected in parallel to each other as shown in Figure7. A subsystem is created selecting the orifices and with the parameters of orifices defined in the Mask of the subsystem as shown in Figure. 5.

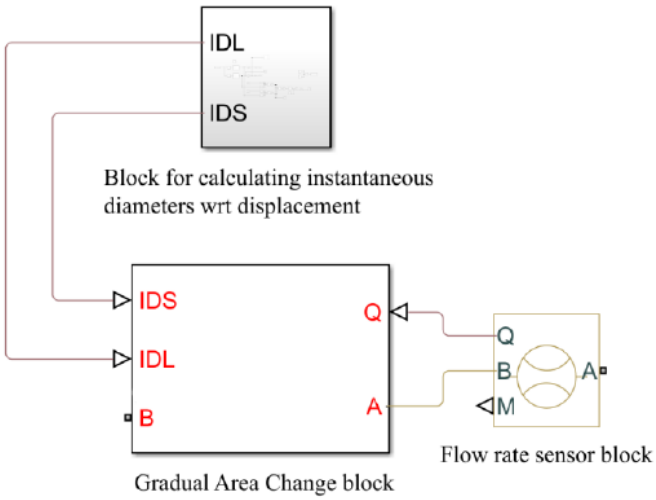

Figure 8: Simscape Gradual Area Change block

Gradual Area Change Region: The conical region, near the inclined orifice has gradually varying area and it is modelled with a custom Simscape component based on Gradual Area Change (GAC) Block. The GAC block is based on the Local Resistance block. The GAC block is bidirectional and computes pressure loss for both the direct flow (gradual enlargement) and return flow (gradual contraction). As mentioned earlier, the diameter of the control rod varies with respect to length. As a result, the cross-sectional area at the inlet and outlet of the gradual area change region also varies as

the piston moves. To calculate the cross-section area at the inlet and outlet of the gradual area change region at a particular instant, the instantaneous diameters corresponding to displacement output of the piston at is calculated. These instantaneous diameters are sent to Gradual Area Change block as shown in Figure 8.

Variable Area Annular Orifice Region: The annular orifice dimensions are decided by the hole diameter of the piston head (constant) and diameter of the control rod (varies with piston displacement). The control rod diameter varies as the piston moves. Therefore, a component block is used to calculate the instantaneous radius of the annular orifice.

The block calculates the instantaneous value of radius of control rod based on the position of piston and sends it to variable area annular orifice block to calculate the instantaneous pressure drop as shown in Figure 9.

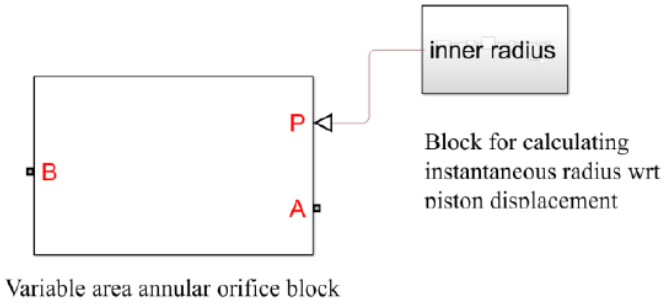

Figure 9: Simscape Variable area annular orifice block

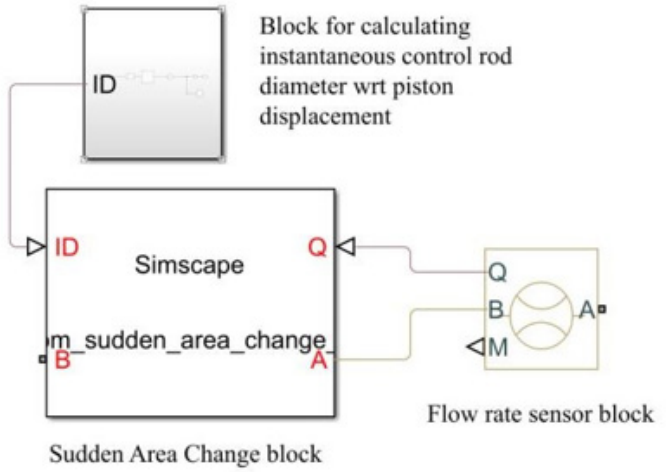

Figure 10: Simscape Sudden Area Change block

Sudden Area Change region: Similar to Gradual Area Change block, the Sudden Area Change block is modelled to account the expansion and contraction of oil flowing out from the annular orifice. Similar to GAC block, the calculated pressure loss co-efficient is then passed on to the local resistance block equation. Since the area change depends on the annular orifice dimensions, the instantaneous control rod diameters are calculated and fed to the Sudden Area Change region block as shown in Figure 10.

Modelling of Dashpot in Simulink/Simscape Fluids

To model the damping effect offered by the dashpot, an Ideal Force Source block is used. It is modelled in such a way that it provides an opposing force against the piston motion at the end of the recuperation stroke to provide a cushioning effect. The force acts only after the piston crosses below l_{pd} and is modelled using a MATLAB function block with appropriate condition statements. The dashpot damping force is calculated using Eq. (23).

$$F_{dps} = \mu\left[\frac{3\pi D_d^3 l_m}{4d_d^3}\left(1+\frac{2d_d}{D_d}\right)\right]\cdot v \qquad (23)$$

Measurement Of Recoil System Parameters in Military Vehicle

The primary objective of the past experiment was to estimate the recoil distance, recoil velocity and transmitted force from the recoil system in selected number of military vehicles during live firing at the Field Firing Range. As the firing occurs, the recoil piston rod, which is attached to the gun breech moves backwards and the entire reciprocating mass translates over the fixed cradle, which in turn is assembled with the trunnion block. The cradle is assembled with a deflector guard in order to protect the crew from the cartridge case, which is ejected out from the breech after firing. The Fig. 11 below shows the schematic of a gun and recoil assembly, which is integrated inside the military vehicle.

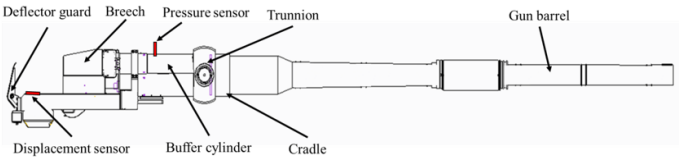

Figure 11: Armament system assembled in the military vehicle

The data such as recoil length versus time and recoil velocity versus time (using tachometer attached rigidly to the cradle) and pressure of the hydraulic fluid in two buffers versus time (using hydraulic pressure transducer connected to a data acquisition system) were captured during the experiment. The sensors have been positioned at the locations which have been indicated in the Figure 11. During each round of firing, the time variant parameters have been captured.

The experiments were conducted on various military vehicles for checking its repeatability with every round of firing and at different gun angles. The transmitted force to the structure is calculated from the above pressure, which is developed in the buffers. The variation of transmitted force has been captured as a function of stroke and has been used as a benchmark of comparison for the present models, since these estimations have been carried out on the actual military vehicle itself.

Results & Discussions

The mathematical model for the tank gun recoil system is developed using MATLAB code and Simscape fluids. The system is modelled as nonlinear 1D, mass, spring and damper system subjected to external force. The firing force acting on the system is evaluated from the experiments. The inertia force is modelled using Newton's second law and recuperator forces are modelled by using helical spring equations. In the MATLAB code model, recoil brake is modelled using the fluid dynamic equations to evaluate the pressure drop and damping across all the orifices during the piston movement. The governing equation of motion is solved to evaluate the acceleration, velocity and displacement of the piston. The force transmitted to the structure during firing is evaluated by summing the forces exerted by

recuperator, recoil brake, dashpot and pressure acting on the piston. In Simscape fluids model, the fluid flow path of the recoil brake is analysed and corresponding hydraulic circuit is modelled using blocks representing different elements of the recoil system. Here the transmitted force is evaluated by using a force sensor block between the system and ground. The results obtained from the models are shown in Figures12, 13, 14.

It is observed that, with the application of firing load, the mass recoils from the initial equilibrium position and its displacement increases. After reaching maximum displacement, the energy stored in the recuperator during recoil phase, forces the mass to the return back to equilibrium position. The mass returns to the initial position without oscillations due to the damping offered by the recoil brake. At the end of recuperation phase, the dashpot provides a cushioning effect by dampening the residual recuperator force available at the end. The transmitted force to the structure increases steeply with the application of firing load and reaches a maximum value. It drops back quickly and finally becomes zero. It is observed that the transmitted force is significantly lesser when compared to the firing force acting on the system proving the fact that the recoil system dissipates the firing loads before transmitting to the structure.

The developed mathematical model has been validated against experimental results, showing strong agreement. The key performance parameters such as maximum recoil displacement, recoil velocity and transmitted force are predicted with acceptable accuracy. The maximum displacement of the recoiling mass during testing was around 349 mm. The maximum displacement predicted by mathematical model developed in MATLAB is 356 mm and that developed using Simscape fluids is 326 mm. The MATLAB and Simscape models show good agreement with experiment with an error of 7 mm and 23 mm in maximum displacement respectively. Similarly, the maximum recoil velocity was found to be 9.32 m/s during testing, while that predicted from the developed mathematical model and Simscape fluids model are 9.24 m/s and 8.92 m/s, respectively and resulting in an error of 0.08 m/s and 0.4 m/s respectively. The maximum transmitted force recorded during testing was 82 tonnes. The force obtained from the developed mathematical model and Simscape fluids model are 82.3 tonnes and 81.8 tonnes repectively, with an error of 0.3 tonnes & 0.2 tonnes respectively. Figure 15 shows the transmitted force variation with respect to recoil distance obtained from the models and experiment. It is clear that both models accurately capture the trend in the variation of transmitted force. This validation confirms that the model is capable of accurately representing the physical system behavior and can be reliably used for further simulation. The developed model will be helpful in understanding of working of existing recoil systems and their effect on the stability of the vehicle. This will serve as foundation in designing and optimizing advanced recoil systems for armoured fighting vehicles.

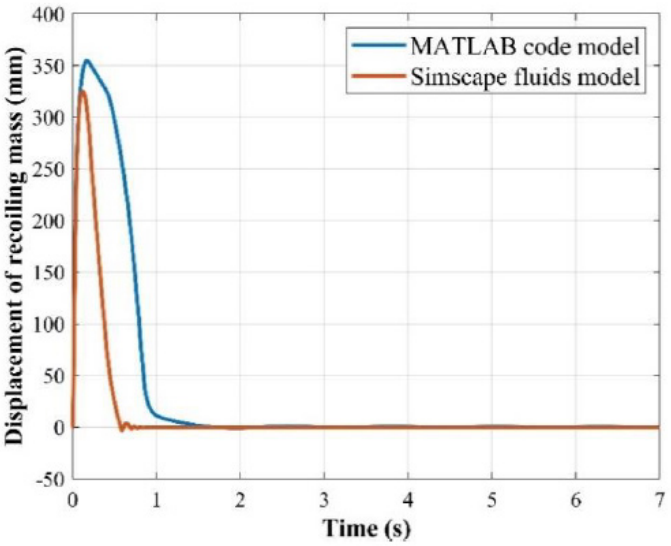

Figure 12: Displacement of recoiling mass

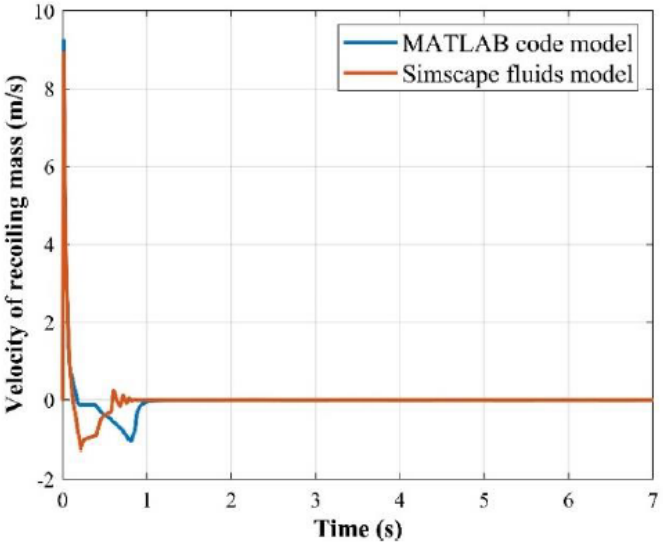

Figure 13: Velocity of recoiling mass

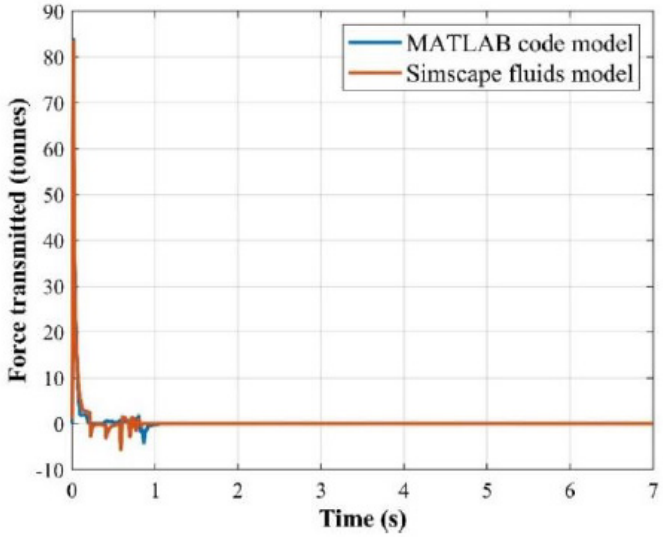

Figure 14: Force transmitted to structure

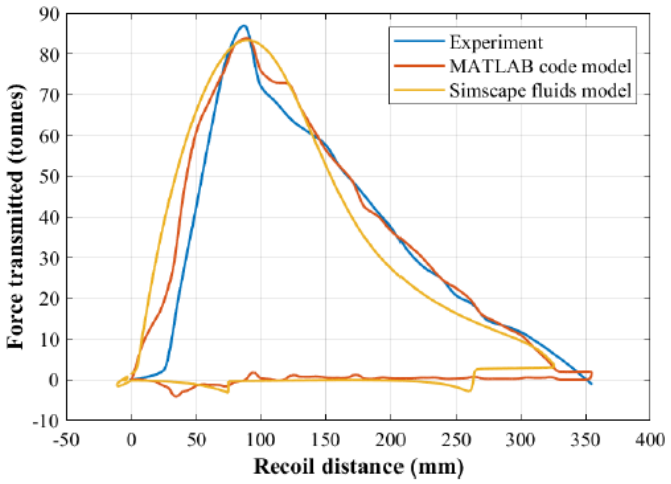

Figure 15: Comparision of force from the models with experiment

It can be seen that the results obtained from developed MATLAB model and Simscape fluids model during the recoil phase are very close. The variations observed between the results during the recuperation phase can be attributed to the difference in modelling of dashpot region. In the Simscape fluids model, due to the assumptions considered and based on the standard available blocksets, the actual flow getting in the dashpot could not be modelled accurately, unlike the customization which was possible in the MATLAB code. Hence, the developed mathematical model by using MATLAB code, yields closer results to experimental findings. In this work, laminar, one-dimensional flow with negligible friction and a constant discharge coefficient was assumed to simplify the governing equations and focus on the principal flow mechanisms. While these assumptions do not fully represent the complex, potentially turbulent conditions observed in high-pressure recoil conditions, the resulting model nonetheless produced predictions in close agreement with experimental data. The assumptions, therefore, provide a reasonable trade-off between analytical simplicity and predictive accuracy. Future work will extend the model to include turbulence and transient effects to broaden its applicability.

Acknowledgments

The authors are very thankful to Utkarsh Chitransh, Technical Officer (CEAD) for providing support in creating schematic of armament assembly and Centre for Engineering Analysis & Design (CEAD) division of CVRDE for their support involved in execution of the above work.

References

1. Lin TY, Ping HC, Yang TY, Chan CT, Yang CC (2009) Dynamic simulation of the recoil mechanism on artillery weapons. ICCES 11:115-122.
2. Turkmen M, Celik HH (2021) Recoil Motion Modeling of a Heavy Weapon with Hydropneumatic Recoil Mechanism. IJSR 10: 1161-1167.
3. Damian Szupieńko, Ryszard WOŹNIAK (2021) Preliminary Physical and Mathematical Model of the Recoil Operated Firearm within the Bolt Recoil Period. Problems of Mechatronics Armament Aviation Safety Engineering 12: 59-74.
4. Yang JM, Yu YN, Shi CM (2023) Modeling and Calculation of Hydraulic Equation of Recoil Brake Which is Unfilled in counterrecoil throttling Chamber. Journal of Physics: Conference Series 2460: 012068.
5. Lai Tuan, Nguyen Phu (2024) Numerical analysis of oil characteristics in hydraulic recoil braking mechanisms. Advanced Engineering Letters 3: 100-109.
6. Tuan NM, Phu NV (2025) Studying the Influence of the Gap between the Recoil Cylinder and Piston on Artillery Operation. JMST Advances 7: 207-216
7. Selim M, Elsaady Wael, Ibrahim Ahmed, Ramy Abdelsalam Ossama (2023) Study of dynamic characteristics of a new suggested recoiling mortar system. Journal of Physics Conference Series 2616: 012012.
8. Roy AK, Lankennavar PH, Ghadge VS (2017) Present and Futuristic Trends in Weapon System. Defence Science Journal 67: 367-374.

Appendix A: Equations for calculating spring stiffness

$$k = \frac{Gd^4}{8D^3n} \qquad (A1)$$

$$K = \sum_{j=1}^{2} \frac{1}{k_j} \qquad (A2)$$

Appendix B: Equations for calculating pressure drop across orifices

$$\Delta p_1 = \rho\left((1+fr)\left(\frac{A_{f1}}{n_{o1}A_{o1}C_d}\right)^2 - 1\right)\frac{v^2}{2} = \rho\left((1+fr)\left(\frac{\frac{\pi}{4}D_t^2 - \pi r_{p1}^2}{n_{o1}\frac{\pi r_{o1}^2}{2}C_d}\right)^2 - 1\right)\frac{v^2}{2} \qquad (B1)$$

$$\Delta p_2 = \rho\left((1+fr)\left(\frac{A_{f2}}{n_{o2}A_{o2}C_d}\right)^2 - 1\right)\frac{v^2}{2} = \rho\left((1+fr)\left(\frac{\frac{\pi}{4}D_t^2 - \pi(r_{p6})^2}{n_{o2}\,\pi r_{on2}^2\,C_d}\right)^2 - 1\right)\frac{v^2}{2} \qquad (B2)$$

where $r_{on2} = r_{o2}\sin(\theta)$

$$\Delta p_3 = 8\mu l_o v\left(\frac{r_{p4}^2 - r_{c1}^2 - 3x^2(\tan\alpha)^2 - 4r_{c1}x(\tan\alpha)}{r_{p3}^4 - r_{c1x}^4 - \frac{\left(r_{p3}^2 - r_{c1x}^2\right)^2}{\log\left(\frac{r_{p3}}{r_{c1x}}\right)}}\right) \qquad (B3)$$

where

$$\alpha = tan^{-1}\left(\frac{r_{c2} - r_{c1}}{l_o}\right);\ r_{c1x} = r_{c1} + x\tan(\alpha)$$

$$\Delta p_4 = \rho\left((1+fr)\left(\frac{A_{f4}}{n_{o3}A_{o3}C_d}\right)^2 - 1\right)\frac{v^2}{2} = \rho\left((1+fr)\left(\frac{\pi r_{p3}^2}{n_{o3}\frac{\pi r_{o3}^2}{2}C_d}\right)^2 - 1\right)\frac{v^2}{2} \qquad (B4)$$

$$\Delta p_5 = \rho\left((1+fr)\left(\frac{A_{f5}}{n_{o3}A_{o3}C_d}\right)^2 - 1\right)\frac{v^2}{2} = \rho\left((1+fr)\left(\frac{\pi r_{p4}^2}{n_{o3}\frac{\pi r_{o3}^2}{2}C_d}\right)^2 - 1\right)\frac{v^2}{2} \qquad (B5)$$

$$\Delta p_6 = 8\mu l_m v\left(\frac{r_{p3}^2 - r_{m1}^2}{r_{m2}^4 - r_{m1}^4 - \frac{\left(r_{m2}^2 - r_{m1}^2\right)^2}{\log\left(\frac{r_{m2}}{r_{m1}}\right)}}\right) \qquad (B6)$$

$$\Delta p_7 = \rho\left((1+fr)\left(\frac{A_{f7}}{\pi A_{o7}C_d}\right)^2 - 1\right)\frac{v^2}{2} = \rho\left((1+fr)\left(\frac{\pi r_{p7}^2}{\left(\pi(r_{p5}^2 - r_{cm}^2)C_d\right)}\right)^2 - 1\right)\frac{v^2}{2} \qquad (B7)$$

$$\Delta p_8 = \rho\left((1+fr)\left(\frac{A_{f8}}{n_{o2}A_{o2}C_d}\right)^2 - 1\right)\frac{v^2}{2} = \rho\left((1+fr)\left(\frac{\pi r_{p4}^2}{n_{o2}\,\pi r_{on2}^2\,C_d}\right)^2 - 1\right)\frac{v^2}{2} \qquad (B8)$$

where $r_{on2} = r_{o2}\sin(\theta)$

$$\Delta p_9 = \rho\left((1+fr)\left(\frac{A_{f9}}{n_{o1}A_{o1}C_d}\right)^2 - 1\right)\frac{v^2}{2} = \rho\left((1+fr)\left(\frac{\frac{\pi}{4}D_t^2 - \pi r_{pe}^2}{n_{o1}\frac{\pi r_{o1}^2}{2}C_d}\right)^2 - 1\right)\frac{v^2}{2} \qquad (B9)$$

$$\Delta p_{10} = \rho\left((1+fr)\left(\frac{A_{f10}}{n_{o3}A_{o3}C_d}\right)^2 - 1\right)\frac{v^2}{2} = \rho\left((1+fr)\left(\frac{\pi r_{p3}^2}{n_{o3}\frac{\pi r_{o3}^2}{2}C_d}\right)^2 - 1\right)\frac{v^2}{2} \quad (B10)$$

$$\Delta p_{11} = 8\mu l_{pd} v\left(\frac{r_{p8}^2 - r_{m1}^2}{r_{p8}^4 - r_{m1}^4 - \frac{\left(r_{p8}^2 - r_{m1}^2\right)^2}{\log\left(\frac{r_{p8}}{r_{m1}}\right)}}\right) \quad (B11)$$